

## OSCILLATORY THERMOCAPILLARY CONVECTION

Jieyong Xu and Abdelfattah Zebib  
Department of Mechanical and Aerospace Engineering  
Rutgers University  
Piscataway, NJ08855-0909

### ABSTRACT

Stability analysis of thermocapillary convection in rectangular cavities is performed using direct numerical simulations. Influence of the Reynolds number( $Re$ ), the fluid Prandtl number( $Pr$ ) and cavity aspect ratio( $Ar$ ) on the motion is investigated. Neutral stability curves for transition to time-dependent convection are delineated in the  $Re - Ar$  plane for fluids with  $Pr=1.0, 4.4, 6.78$  and  $10$ . Several interesting features of these diagrams are discussed. One important conclusion is that  $Ar_{cr}$  increases as  $Pr$  decreases. Thus, large values of both  $Ar$  and  $Re$  are necessary to induce thermocapillary oscillations for small  $Pr$  fluids such as liquid metals and semiconductor melts. Energy analysis is also performed for the oscillatory flow in the neighborhood of critical points in order to gain insight into the mechanisms leading to instability.

### INTRODUCTION

Understanding fluid motion is crucial in some material processing technologies. In crystal growth from the melt, single crystals with uniform material properties are desired, but homogeneity in crystals can be destroyed if melt motion is unsteady [1]. In the terrestrial environment, buoyancy and thermocapillarity are two major causes for convection. However, in low gravity environment, thermocapillary convection becomes dominant[2].

Numerous experiments (for example, [3], [4] and [5]) have demonstrated the existence of instability of thermocapillary convection, i.e. when the Marangoni number( $Ma$ ) exceeds a critical value, the motion undergoes a transition from steady to oscillatory.

Thermocapillary flows have received considerable interest. A rich body of numerical investigations are available in the literature (see [6], [7] and [8]). Results of direct numerical simulation of oscillatory thermocapillary convection was reported in [9] by Peltier & Biringen. They provided a stability diagram in the  $(Ar, Ma)$  space for a  $Pr=6.78$  fluid, and found a minimum critical  $Ar$  near 2.3 and a minimum critical  $Ma$  near 20,000 within the parameter range of  $Ar \leq 3.8$ .

Discussions of instability mechanisms can be found in [10] and [11] for dynamic thermocapillary infinite liquid layers, and in [12] for thermocapillary liquid bridges. Description of the oscillatory instability is also provided in [9], relating the temporal evolution of large-scale structures in the flow and their interaction with the temperature sensitive free surface.

Here, we present a detailed stability diagram for fluids with  $Pr=10.0, 6.78, 4.4$  and  $1.0$ . Interesting features in the diagram are discussed. Comparison of flow patterns is provided to investigate the influence of  $Re$  and  $Ar$  on the motion of a  $Pr=10$  fluid. In addition, energy analysis results are also given for convection of a  $Pr=4.4$  fluid with  $Re$  near both higher and lower critical points of the unstable region at  $Ar=3.0$ .

## MODEL DESCRIPTION AND NUMERICAL PROCEDURE

The physical model considered is thermocapillary convection of incompressible and Newtonian fluid in a rectangular cavity with height  $H$  and width  $Ar \times H$  ( $Ar$  is the aspect ratio). Two vertical isothermal side walls are kept at  $T_h$  on the left and  $T_c$  on the right, respectively. Bottom boundary is rigid and adiabatic. Top boundary is a flat free surface open to a passive gas. Here, surface tension on the free surface is assumed to be a linear function of temperature as  $\sigma = \sigma_0 - \gamma(T - T_0)$ .

A dimensionless mathematical model in the stream function - vorticity formulation is used for numerical simulation, in which length, temperature, velocity and time are made dimensionless by use of scales  $H$ ,  $\Delta T = (T_h - T_c)$ ,  $\gamma \Delta T / \mu$  and  $H^2 / \nu$ , respectively. Dimensionless parameters are defined as:  $Pr = \frac{\mu}{\alpha}$  and  $Re = \gamma \frac{\Delta T H}{\mu \nu}$ , where  $\mu$ ,  $\nu$  and  $\alpha$  are dynamic viscosity, kinematic viscosity and thermal diffusivity, respectively.

The coupled equation system is solved by a finite volume based scheme, in which the Poisson equation for the stream function is solved by the SOR method. Both the vorticity transport and energy equations are solved by the alternating direction implicit (ADI) method. All time derivatives and spatial derivatives including boundary conditions are approximated in second order accuracy. Velocities are obtained as spatial derivatives of stream function. Uniform mesh is used in the solution procedure with mesh resolution of 50 to 90 points per dimensionless unit length, depending on the Reynolds number considered.

## RESULTS

For thermocapillary convection of a  $Pr=6.78$  fluid in rectangular cavities, Peltier & Biringen [9] constructed a stability diagram in the  $(Ar, Ma)$  plane for the region  $Ar \leq 3.8$  and  $Ma \leq 1.0 \times 10^5$ . Their  $Ma$  is equivalent to our  $RePrAr$ . Some interesting characteristics were found, including the existence of double valued stability limits, i.e. as  $Ma$  goes up, the flow first changes from stable to oscillating at  $Ma_{cr1}$ , and then becomes stable again when  $Ma_{cr2}$  is reached.  $Ma_{cr2}$  grows monotonically with  $Ar$ , however,  $Ma_{cr1}$  does not.

In the present work, we extend this investigation to fluids with  $Pr=1.0, 4.4$  and  $10.0$ , and construct the stability diagrams in the  $(Ar, Re)$  plane. A wider range of parameter space ( $0.0 \leq Ar \leq 7.0$  and  $0.0 \leq Re \leq 1.3 \times 10^4$ ) is considered as shown by Fig. 1, in which more interesting features are found. If we look at the particular fluid with  $Pr=4.4$ , the first critical aspect ratio is around 2.6. Unstable region exists for any  $Ar > 2.6$ , and more interestingly, there are more than one unstable regions with  $Ar > 6.0$ , i.e. if  $Re$  goes up from zero, one can find that the flow is steady at low  $Re$ , starts to oscillate at first critical point, goes back to steady state at second critical point, and becomes oscillatory again as  $Re$  reaches its third critical point. In addition, stability curves of fluids with different  $Pr$  do not cross each other. Neutral curves of smaller  $Pr$  fluids always locate inside curves of larger  $Pr$ , i.e. when  $Pr$  goes smaller, the critical aspect ratio always becomes larger, so does the lowest critical Reynolds number. From the trend given by these curves, we can draw a very important conclusion that, for fluids with very low  $Pr$ , large values of critical  $Ar$  and  $Re$  are expected for the transition to oscillatory thermocapillary convection.

The convective flow field is strongly influenced by  $Re$ ,  $Ar$  and  $Pr$ . For a  $Pr=10$  fluid, Fig. 2 gives three examples of streamlines at  $Ar=3.0$  and  $Ar=6.0$ . (a) shows the flow field at  $Re_{cr1}$  for  $Ar=3.0$ , in which one can see a bi-cellular structure with a stronger cell near the hot wall and a much weaker cell close to the cold wall. Increasing  $Re$  to  $Re_{cr2}$  at about 7400, one can find, in (b), that the previous strong hot wall cell moves to the center of the cavity, and the weak cell disappears. For a larger aspect ration ( $Ar=6.0$ ), Fig. 2 (c) exhibits the flow pattern at  $Re_{cr1}$ , from which we find that three cells exist, with the strongest one

still near the hot wall. Further increase of  $Ar$  will result in more cellular structure in the flow field.

For convection of a  $Pr=10$  fluid at a large aspect ratio ( $Ar=20$ ), Fig. 3 displays the mean velocity profiles and snapshots of temperature fluctuation fields for three different values of  $Re=1012$ ,  $1025$  and  $1500$ , respectively. Comparison of these three mean velocity profiles shows almost identical patterns even when  $Re$  changes from  $1012$  to  $1500$ , with most strong activities locating near two side walls. However, large difference can be found among the temperature fluctuation fields. At  $Re=1012$  (b-1), which is very close to  $Re_{cr1}$ , a *thermal wave* generates near the center of the cavity and starts to die at the right edge of the strong flow cell near the hot wall. Most area in the right part of the cavity remains pretty calm. The *wave* actually propagates toward the hot wall if we look at snapshots at different time instants, which is in agreement with [10]. As  $Re$  goes up a little bit to  $1025$ , (b-2) shows that the starting point of the *thermal wave* moves toward the cold wall. Further increase  $Re$ , this starting point keeps moving to the right until it reaches the cold wall. Fig. (b-3) shows the case when  $Re=1500$ , in which one can see a *wave* generating at the cold wall, propagating actively, and dying at the right edge of the strong flow cell near the hot wall.

### ENERGY ANALYSIS

Energy analyses are performed for flows with Reynolds numbers in the neighborhoods of different critical points. The physical parameters of the oscillatory flows are decomposed into their mean and fluctuating components, and investigations are conducted on the behavior of the fluctuation kinetic energy ( $k$ ) and the fluctuation thermal energy ( $\theta = t^2/2$ ).

For the case  $Ar=3.0$  and  $Pr=4.4$ , results of the energy analysis are provided here for flows with Reynolds numbers near both lower ( $Re=1950$ ) and higher ( $Re=5020$ ) critical points of the unstable region. Temporal variations over one flow oscillation period are shown in Fig. 4(a-1) and (a-2) for the rate of change of the total fluctuation kinetic energy ( $dK/d\tau = \frac{d}{d\tau}(\int k d\Omega)$ ), as well as its components  $I_{k_1}$  (production),  $I_{k_2}$  (diffusion) and  $I_{k_3}$  (dissipation). It is seen that  $dK/d\tau$  oscillates with its time average being equal to zero, which means no kinetic energy is added to the flow over each period of oscillation. This is consistent with the fact that the flow field oscillates with a stable amplitude. If we look at  $I_{k_1}$ ,  $I_{k_2}$  and  $I_{k_3}$ , we find  $I_{k_1}$  and  $I_{k_3}$  providing two major contributions, with  $I_{k_1}$  always being positive (destabilizing) and  $I_{k_3}$  always being negative (stabilizing). Time averages of  $I_{k_1}$  and  $I_{k_3}$  are much larger than that of  $I_{k_2}$ , however, the phase difference between  $I_{k_1}$  and  $I_{k_3}$  is always near  $\pi$ , which means that  $I_{k_3}$  always cancels the effect of  $I_{k_1}$ . This gives the smaller term  $I_{k_2}$  a chance to influence the temporal behavior of  $dK/d\tau$ . In Fig. 4(a-2), which is for the higher critical point, one can clearly see that  $dK/d\tau$  oscillates at a very close amplitude and a very small phase difference with  $I_{k_2}$ , while the phase difference between  $I_{k_1}$  and  $I_{k_3}$  is almost  $\pi$ .

Variation of the rate of change of the total fluctuation thermal energy ( $d\Theta/d\tau = \frac{d}{d\tau}(\int \theta d\Omega)$ ) and its components ( $I_{t_1}$  and  $I_{t_2}$ ) are given in Fig. 4(b-1) and (b-2) for the lower and higher critical points, respectively. As expected,  $d\Theta/d\tau$  oscillates with its time average being equal to zero, since the temperature field oscillates in a limit cycle with stable amplitude. In addition, although the time averages of  $I_{t_1}$  and  $I_{t_2}$  have the same absolute value, the oscillation amplitude of  $I_{t_1}$  is much larger than that of  $I_{t_2}$ . Thus  $I_{t_1}$  dominates the oscillatory behavior of  $d\Theta/d\tau$ . In both cases, the phase difference between  $I_{t_1}$  and  $d\Theta/d\tau$  is very small. If we further compare the magnitude of the destabilizing fluctuation thermal energy component ( $I_{t_1}$ ) and the kinetic energy components ( $I_{k_1}$  and  $I_{k_2}$ ), we find that the magnitude of thermal energy production  $I_{t_1}$  is generally two to three orders larger than that of  $I_{k_1}$  or  $I_{k_2}$ . Thus,  $I_{t_1}$  appears to be the major driving source of flow instability.

## CONCLUSIONS

Direct numerical simulation is employed for stability analyses of thermocapillary driven convection in rectangular cavities. Stability boundaries are delineated in the  $Re - Ar$  plane, in which several interesting features are found. Influence of  $Re$  and  $Ar$  on the flow patterns and the temperature fields is briefly discussed. In addition, energy analyses are performed to gain insight into mechanisms involved in the onset of instability. Results are presented for a  $Pr=4.4$  fluid with  $Re$  near both higher and lower critical points at  $Ar=3.0$ . Investigations on 2D and 3D convection of lower  $Pr$  as well as larger  $Ar$  and  $Re$  are in progress.

## ACKNOWLEDGEMENT

This research is sponsored by NASA through grant No. NAG3-1453. We also acknowledge the Pittsburgh Supercomputing Center for providing CRAY C90 time through grant No. CTS950032P.

## References

- [1] Hurle, D. T. J. *Thermo-hydrodynamic oscillation in liquid metals: the cause of impurities striations in melt-grown crystals*. J. Phys. Chem. Solids, Suppl. no.1, 659-669(1967).
- [2] Ostrach, S. *Low-gravity fluid flows*. Ann. Rev. Fluid Mech., **14**, 313-345(1982).
- [3] Chun, C. H. and Wuest, W. *Experiments on the transition from the steady to the oscillatory Marangoni convection of a floating zone under reduced gravity effect*. Acta Astronautica, **6**, 1073-1082(1979).
- [4] Chun, C. H. *Experiments on the transition from the steady to the oscillatory temperature distribution in a floating zone due to Marangoni convection*. Acta Astronautica, **7**, 479-488(1980).
- [5] Preisser, F., Schwabe, D., and Scharmann, A. *Steady and oscillatory thermocapillary convection in liquid columns with free cylindrical surface*. J. Fluid Mech., **126**, 545-567(1983).
- [6] Zebib, A., Homsy, G. M. and Meiburg, E. *High Marangoni number convection in a square cavity*. Physics Fluids, **28**(12), 3467-3476(May 1985).
- [7] Carpenter, Bradley M. and Homsy, G. M. *High Marangoni number convection in a square cavity: Part II*. Physics Fluids A, **2**(2), 137-149(1990).
- [8] Ben Hadid, H. and Roux, B. *Thermocapillary convection in long horizontal layers of low-Prandtl number melts subject to horizontal temperature gradient*. J. Fluid Mech., **221**, 77-103(1990).
- [9] Peltier, L. J. and Biringen S. *Time-dependent thermocapillary convection in a rectangular cavity: numerical results for a moderate Prandtl number fluid*. J. Fluid Mech., **257**, 339-357(1993).
- [10] Smith, Marc K. and Davis, Stephen H. *Instabilities of dynamic thermocapillary liquid layers. Part 1. Convective instabilities*. Physics Fluids, **132**, 119-144(1983).
- [11] Smith, Marc K. *Instability mechanisms in dynamic thermocapillary liquid layers*. Physics Fluids, **29**(10), 3182-3186(1986).
- [12] Wanschura, M., Shevtsova, V. M., Kuhlmann, H. C. and Rath, H. J. *Convective instability mechanisms in thermocapillary liquid bridges*. Physics Fluids, **7**(5), 912-925(May 1995).
- [13] Braunsfurth, M. G. and Homsy, G. M. *Experimental study of buoyant-thermocapillary convection in a rectangular cavity*. 48th annual meeting of APS-DFD, (presentation FG3), (1995).

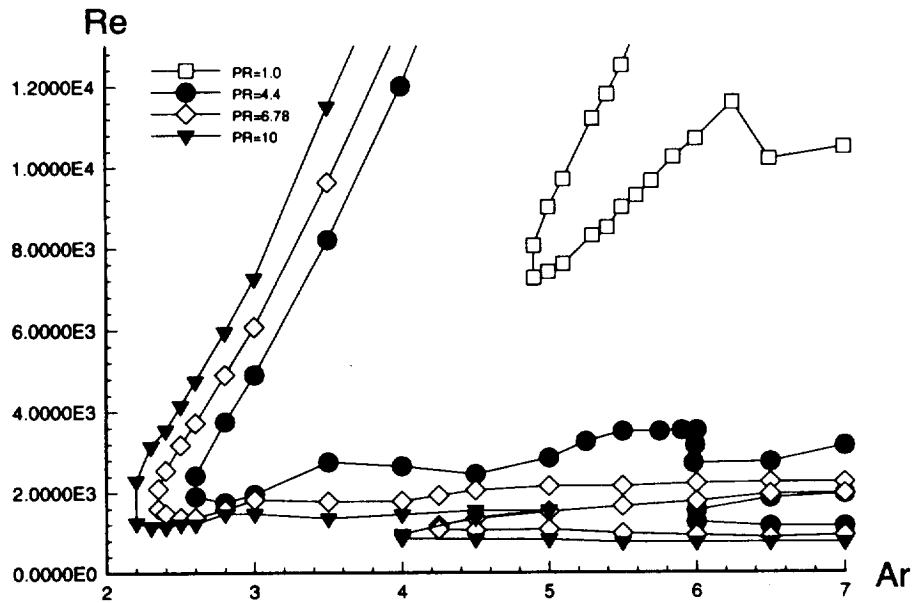


Figure 1: Stability diagrams in the Re - Ar plane for fluids with Pr=10.0, 6.78, 4.4 and 1.0.

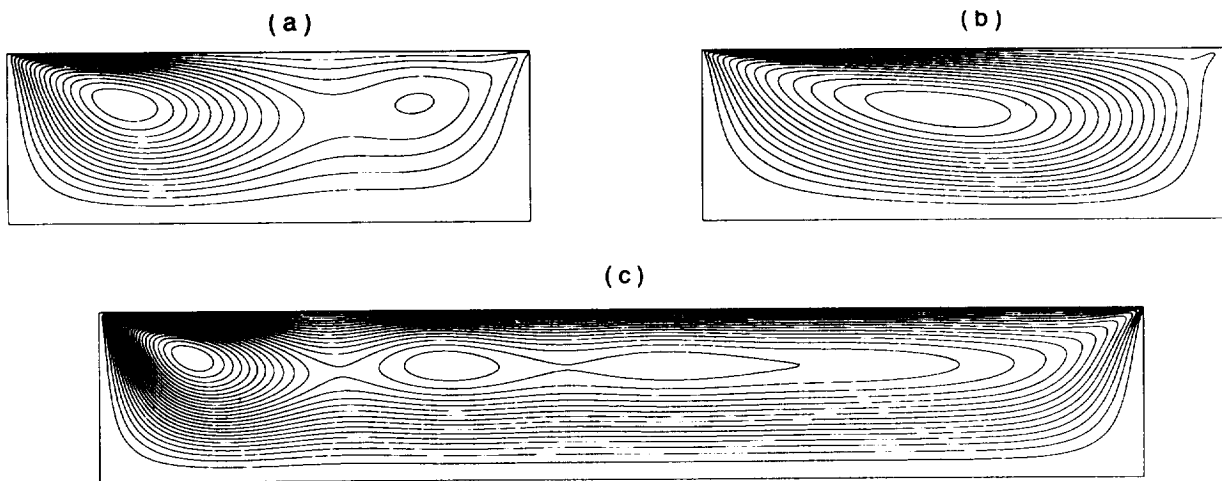


Figure 2: Examples of streamlines for convection of a Pr=10 fluid. Case (a): Ar=3.0, Re=1530 ( $\approx$  the first critical number); Case (b): Ar=3.0, Re=7400 ( $\approx$  the second critical number); Case (c): Ar=6.0, Re=700 ( $\approx$  the first critical number).

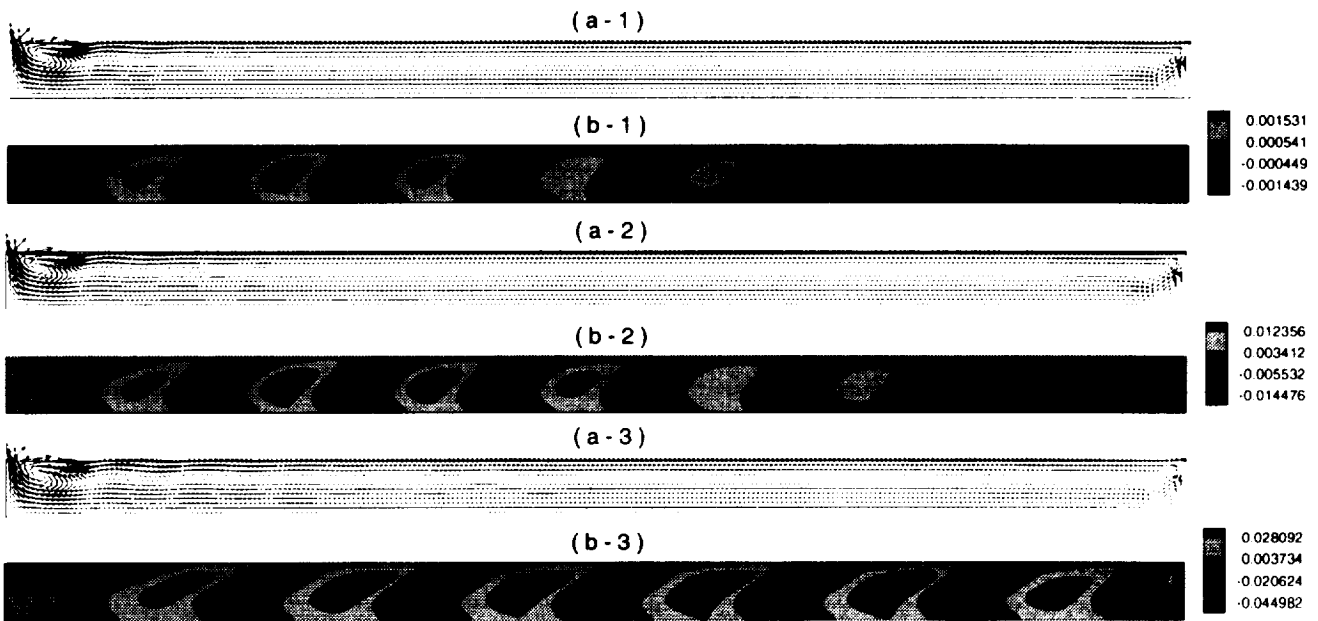


Figure 3: Comparison of mean velocity profiles and temperature fluctuation fields of a  $Pr=10$  fluid at large aspect ratio  $Ar=20$ . Case 1:  $Re=1012$ , which is approximately the first critical point; Case 2:  $Re=1025$ , which is slightly higher than the first critical point; Case 3:  $Re=1500$ , which is much higher than the first critical point.

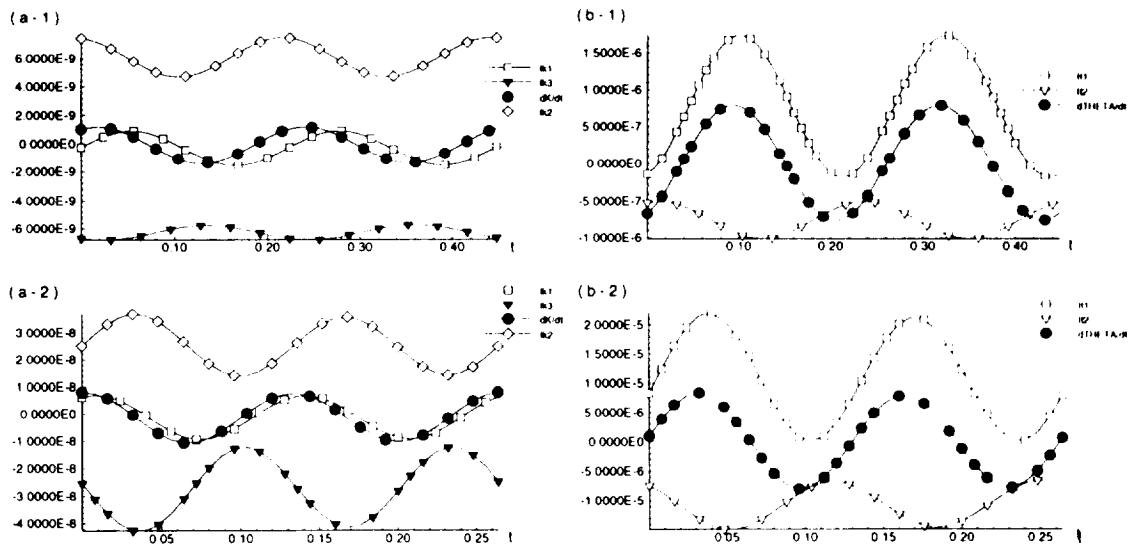


Figure 4: Temporal variation of the rate of change of the total kinetic energy  $\frac{dK}{dr}$ , the thermal energy  $\frac{d\Theta}{dr}$  and their components  $I_{k_1}$ ,  $I_{k_2}$ ,  $I_{k_3}$ ,  $I_{t_1}$  and  $I_{t_2}$  for a  $Pr=4.4$  fluid at  $Ar=3.0$ . (a-1) and (b-1) give results for  $Re=1950$  (near the lower critical point), (a-2) and (b-2) provide results for  $Re=5020$  (near the higher critical point).